Catalase-Peroxidase (*Mycobacterium tuberculosis* KatG) Catalysis and Isoniazid Activation†

Salem Chouchane,‡ Istvan Lippai,§ and Richard S. Magliozzo*,‡

Department of Chemistry, Brooklyn College CUNY, 2900 Bedford Avenue, Brooklyn, New York 11210-2889, and Department of Physiology & Biophysics, Albert Einstein College of Medicine of Yeshiva University, 1300 Morris Park Avenue, Bronx, New York 10461

Received March 14, 2000; Revised Manuscript Received May 24, 2000

ABSTRACT: Resonance Raman spectra of native, overexpressed *M. tuberculosis* catalase-peroxidase (KatG), the enzyme responsible for activation of the antituberculosis antibiotic isoniazid (isonicotinic acid hydrazide), have confirmed that the heme iron in the resting (ferric) enzyme is high-spin five-coordinate. Difference Raman spectra did not reveal a change in coordination number upon binding of isoniazid to KatG. Stopped-flow spectrophotometric studies of the reaction of KatG with stoichiometric equivalents or small excesses of hydrogen peroxide revealed only the optical spectrum of the ferric enzyme with no hypervalent iron intermediates detected. Large excesses of hydrogen peroxide generated oxyferrous KatG, which was unstable and rapidly decayed to the ferric enzyme. Formation of a pseudo-stable intermediate sharing optical characteristics with the porphyrin π-cation radical−ferryl iron species (Compound I) of horseradish peroxidase was observed upon reaction of KatG with excess 3-chloroperoxybenzoic acid, peroxyacetic acid, or *tert*-butylhydroperoxide (apparent second-order rate constants of 3.1×10^4, 1.2×10^4, and 25 M^{-1} s^{-1}, respectively). Identification of the intermediate as KatG Compound I was confirmed using low-temperature electron paramagnetic resonance spectroscopy. Isoniazid, as well as ascorbate and potassium ferrocyanide, reduced KatG Compound I to the ferric enzyme without detectable formation of Compound II in stopped-flow measurements. This result differed from the reaction of horseradish peroxidase Compound I with isoniazid, during which Compound II was stably generated. These results demonstrate important mechanistic differences between a bacterial catalase-peroxidase and the homologous plant peroxidases and yeast cytochrome *c* peroxidase, in its reactions with peroxides as well as substrates.

Isoniazid (isonicotinic acid hydrazide, INH)[1] is a first-line antibiotic used against *Mycobacterium tuberculosis* infections since 1952 (*1*). The mode of action of isoniazid is not fully understood, but evidence that certain isoniazid-resistant strains of mycobacteria have reduced catalase-peroxidase (KatG) enzyme activity (*2*) suggested that the antibiotic is acted upon by this enzyme and, therefore, that isoniazid is a prodrug (*3*−*5*). There followed a demonstration that expression of KatG is a requirement for bacterial sensitivity to isoniazid (*3, 6*) and that the principal mechanism of INH resistance in clinical isolates may involve loss of KatG function due to mutations in the *katG* gene (*7*−*11*).

Catalase-peroxidase is a heme protein encoded by the *katG* gene and is found in many microorganisms, most of which are not especially sensitive to isoniazid. A broad range of studies has therefore been directed at explaining the chemistry and biology of isoniazid action, including a search for a mycobacterial target of drug action. Such a target was suggested by the finding of drug resistance in *M. tuberculosis* strains that do not carry a mutation in *katG*, but are *inhA* mutants, and by in vitro studies of InhA enzymology (*12*−*15*). The InhA protein is a fatty acyl carrier protein-enoyl reductase, which functions in the mycolic acid biosynthetic pathway in mycobacteria. A three-dimensional X-ray crystallographic study of InhA identified an acyl-NADH adduct derived from isoniazid as the species likely to be responsible for the irreversible inhibition of this enzyme's activity. This adduct was formed by manganese-catalyzed oxidations occurring in the presence of isoniazid, NADH, and the reductase (*16*). Another enzyme, which is a β-ketoacyl acyl-carrier protein synthase, has also been suggested to be a target of isoniazid action in *M. tuberculosis* according to metabolic and other studies (*17*).

The association between KatG enzyme activity and drug efficacy is well established, though certain questions about the target(s) and chemical mechanism of isoniazid "activation" remain under investigation. The *M. tuberculosis* KatG enzyme has homology to yeast cytochrome *c* peroxidase (CCP) and to plant peroxidases, though it is twice the length of these peroxidases as a result of gene duplication (*18*). There is high sequence homology to CCP in both the first and second halves of the KatG polypeptide, but only one

† This work was supported by National Institutes of Health Grant AI-43582 (NIAID).

* To whom correspondence should be addressed. E-mail: rmaglioz@brooklyn.cuny.edu.

‡ Brooklyn College CUNY.

§ Albert Einstein College of Medicine of Yeshiva University.

[1] Abbreviations: KatG, catalase-peroxidase; INH, isonicotinic acid hydrazide; HRP, horseradish peroxidase; CCP, cytochrome *c* peroxidase; tBOOH, *tert*-butyl hydroperoxide; CPBA, 3-chloroperoxybenzoic acid; PAA, peroxyacetic acid; BHA, benzhydroxamic acid.

10.1021/bi0005815 CCC: $19.00
Published on Web 07/14/2000

heme binding consensus sequence is found per polypeptide (in the N-terminal half). The optical absorption spectra of catalase-peroxidases exhibit low ratios for the Soret region absorbance (near 407 nm) compared to the absorbance at 280 nm, which has led to the supposition that these multimeric enzymes contain heme in only half the heme binding sites. This misconception is corrected in the present manuscript.

Questions remain about the identity of an activated form(s) of isoniazid responsible for its bacteriocidal effect, and, also, which oxidation states of catalase-peroxidase are catalytically competent to produce this activation. By analogy to classical peroxidases, hydrogen peroxide might be considered to be required for initiating peroxidative drug activation in a pathway beginning from the resting enzyme. In the typical peroxidase cycle operating in the oxidation of organic molecules by HRP, for example (*19*, *20*), the resting enzyme reacts with 1 equiv of H_2O_2 to give Compound I (Cmpd I), an oxyferryl iron-protoporphyrin IX:π-cation radical. Reduction of Cmpd I by a single electron yields a second intermediate, Compound II (Cmpd II), which contains an oxyferryl heme but with no cation radical. Finally, Cmpd II can be reduced to the ferric state of the resting enzyme by another single-electron step (*21*−*23*). In CCP, the second oxidizing equivalent removed by hydrogen peroxide is not stabilized in the porphyrin π-cation radical, but resides instead on a tryptophan radical lying near the heme group (*24*−*26*). This species is known as Compound ES (Cmpd ES). Another oxidation state that may have catalytic relevance in certain peroxidase reactions is the oxyferrous form known as Compound III (Cmpd III) (*27*).

M. tuberculosis KatG is a dimer of 80 kDa subunits whose homology to HRP and CCP, especially in the distal and proximal heme regions, raises the likelihood that reaction with peroxide leads to the formation of hypervalent intermediates related to Cmpds I or ES. Cmpd I is a required intermediate in the catalytic cycle of peroxidases. The possibility that Cmpd ES may be formed is also considered since there is a conserved tryptophan in KatG analogous to the one carrying the radical in CCP Cmpd ES (*26*, *28*). The stabilization of the various intermediates, including Cmpd I and/or Cmpd ES, Cmpd II, and Cmpd III (*29*−*31*), has been clearly established for many peroxidases but not for mycobacterial KatG, nor has there been a direct demonstration of the chemical mechanism for drug activation or for the steps that follow. [A recent report (*32*) on the KatG from the cyanobacterium *Synechocystis* presented optical evidence for species identified as Cmpds I and II, though the spectral features seem to differ from those characterized in other peroxidases.] Evidence has been presented for initiation of isoniazid oxidation in the presence of the resting enzyme, oxygen, and a reductant, apparently without Cmpd I involvement (*33*). Isoniazid oxidation also occurs in the presence of KatG and superoxide anion (*34*). Oxidative activation of INH may also be mediated nonenzymatically, by Mn(III), which can be generated via the low-level manganese peroxidase activity exhibited by *M. tuberculosis* catalase-peroxidase (*35*).

In our efforts to characterize KatG and its reaction(s) with INH, we have undertaken optical stopped-flow spectrophotometric studies of the purified, overexpressed *M. tuberculosis* enzyme. We present optical and EPR evidence for formation of Cmpd I in *M. tuberculosis* KatG and evidence that Cmpd I reacts very rapidly with INH. EPR, resonance Raman, and optical spectroscopies were used to characterize the purified enzyme and some of the intermediates. The kinetics of reaction of the resting enzyme with various peroxides are analyzed and compared to similar reactions using HRP.

EXPERIMENTAL PROCEDURES

Materials. E. coli UM262 pKAT II (overexpression system containing *M. tuberculosis KatG* gene) was a gift from Stewart Cole (Institue Pasteur, Paris, France). Horseradish peroxidase was purchased from Fluka Biochemicals and was used without further purification. All other reagents were from Sigma-Aldrich, including isonicotinic acid hydrazide (INH), which was recrystallized from methanol before use.

Purification of M. tuberculosis Catalase-Peroxidase. The catalase-peroxidase used in this study was isolated and purified from an overexpression system in *E. coli* strain UM262 (*KatG* minus) expressing the *M. tuberculosis KatG* gene. The enzyme was purified by FPLC according to a published procedure with minor modification (*36*). The pure enzyme had an optical purity ratio (A_{407}/A_{280}) greater than or equal to 0.66. Spectrophotometric measurements were made using a model NT14 UV−Vis spectrophotometer (Aviv Associates, Lakewood, NJ) interfaced to a personal computer. Protein concentration was determined using the Bio-Rad protein assay reagent (Bradford method) or using the heme extinction $\epsilon_{407\ nm} = 100\ mM^{-1}\ cm^{-1}$. Catalase activity was assayed in phosphate buffer, pH 7.5, using approximately 25 mM H_2O_2, following the decrease in absorbance at 240 nm typically from 0.8 to 0.65 ($\epsilon_{240\ nm} = 43.6\ M^{-1}\ cm^{-1}$) (*37*). One unit of catalase activity is defined as the amount of enzyme catalyzing the decomposition of 1 μmol of H_2O_2/min at 25 °C. Peroxidase activity was measured spectrophotometrically in 50 mM sodium acetate buffer, pH 5.5, using *tert*-butyl hydroperoxide (23 mM) and *o*-dianisidine (0.1 mM), following color development at 460 nm ($\epsilon_{460} = 11.33\ mM^{-1}\ cm^{-1}$) (*36*). One unit of peroxidase activity is defined as the amount of enzyme that catalyzes the oxidation of 1 μmol of *o*-dianisidine/min. SDS gel electrophoresis was carried out under denaturing (SDS−PAGE) and nondenaturing (Native-PAGE) conditions using a Pharmacia Biotech PhastGel system.

The extinction coefficient of heme in the enzyme was determined using the pyridine hemochromogen method (*38*).

Stopped-Flow Optical Measurements. The kinetics of the reaction of KatG with peroxides were measured using a double-mixing stopped-flow apparatus (HiTech Scientific model SF-61DX2) equipped with a rapid scanning diode array spectrophotometer and Kinet-Asyst software for data acquisition and analysis. Potassium phosphate buffer, pH 7.2, was used except where otherwise noted, and all reactions were thermostated at 25 °C. For Cmpd I formation, KatG (20 μM) was loaded into one syringe, and H_2O_2, CPBA, tBOOH, or PAA was loaded into the second syringe. The drive syringes and the reaction cell were equilibrated at 25 °C, and equal volumes of reactants were mixed to initiate reactions. Spectra were acquired from 350 to 700 nm as a function of time to follow the disappearance of the spectrum of the ferric enzyme and the appearance of the new species.

For the purpose of obtaining kinetic parameters, the change in absorbance was monitored at 411 nm, and the data were fit to first-order reaction kinetics. The reaction of Cmpd I with INH or other substrates was followed using a sequential mixing mode: KatG (20 μM) was mixed with CPBA (50 μM) or PAA (200 μM) in the aging loop for 4 s; substrate was then added to the preformed Cmpd I, and spectra were acquired as above. Only the enzyme absorbs in the region observed. For comparison, similar experiments, which monitored Cmpd I formation from hydrogen peroxide, and its reduction to Compound II by INH, were performed using horseradish peroxidase.

Electron Paramagnetic Resonance and Resonance Raman Spectroscopies. Low-temperature EPR spectra were obtained at X-band using a Varian E-12 spectrometer interfaced to a personal computer, and equipped with a liquid helium cryostat and Heli-Tran liquid helium transfer system (Advanced Research Systems, Inc., Allentown, PA). Data acquisition made use of WinEPR software provided by the Research Resource in Pulsed EPR at the Albert Einstein College of Medicine, Bronx, NY. For Cmpd I sample preparation, 40 μM KatG was mixed with 400 μM peroxyacetic acid into the same syringe; after 10 s incubation, the mixture was frozen by expelling the solution directly into liquid nitrogen. The resulting powder was packed into an EPR tube, and the spectrum was recorded at approximately 20 K.

Data Acquisition. Resonance Raman data were provided by Dr. Denis Rousseau, Albert Einstein College of Medicine, Bronx, NY. Excitation was generally at 413 nm, and low power (10 mW) was used to avoid alterations observed during high-power irradiation. Enzyme concentration was approximately 40 μM in potassium phosphate buffer, pH 7.2. The fluoro and cyano forms were produced by addition of excess buffered fluoride or cyanide to the native enzyme. Complete conversion to the six-coordinate forms was confirmed by recording the optical spectrum of the products in the same cuvette used in the Raman spectrometer. Spectra of the resting enzyme in the presence of isoniazid contained 100-fold excess drug relative to heme. Ferrous-CO KatG was prepared by dithionite reduction of resting KatG under anaerobic conditions in the presence of 1 atmosphere of CO gas.

RESULTS

The catalase-peroxidase used in these studies was produced in *E. coli* using an overexpression system carrying the *M. tuberculosis katG* gene. This recombinant enzyme has been reported to be a dimer that contains 1 equiv of heme per dimer based on the low ratio of the Soret absorbance relative to the absorbance in the UV region for the pure enzyme (*39*, *40*). A careful evaluation of the heme extinction coefficient (100 mM^{-1} cm^{-1}) along with a calculation of the extinction at 279−280 nm based on the amino acid composition predicted from the *katG* gene sequence (and confirmation that the overexpressed enzyme is a dimer) leads to the conclusion that the holoenzyme does not lack heme. *M. tuberculosis* KatG contains 24 tryptophans, 26 phenylalanines, and 21 tyrosines, giving a calculated $E_{279} = 164.2$ M^{-1} cm^{-1} (*41*). Other peroxidases (nonbacterial) to which KatG has been compared have much smaller extinction coefficients at 279 nm. For example, HRP (*Armoracia rusticana*), which contains 1 tryptophan, 20 phenylalanines, and 5 tyrosines, has a calculated $E_{279} = 12.9$ M^{-1} cm^{-1} while CCP, which contains 7 tryptophans, 18 phenylalanines, and 14 tyrosines, has a calculated $E_{279} = 58.5$ M^{-1} cm^{-1}. Since both enzymes have similar extinction coefficients for their ferric heme groups, HRP and CCP have much higher optical purity ratios. For *M. tuberculosis* KatG, the optical ratio predicted using the Soret extinction coefficient and the calculated E_{279} is equal to 0.61. This value is close to that for the purest protein we have produced (nearly 0.7). This result demonstrates that the true extinction coefficient at 279 nm is somewhat smaller than the calculated value, but, more importantly, that *M. tuberculosis* KatG expressed in *E. coli* contains 2 hemes/dimer and also that the catalase-peroxidases, in general, are likely to contain 1 heme/monomer in multimers (holoenzymes) containing a full complement of heme groups. The optical ratio for purified wild-type *M. smegmatis* catalase-peroxidase, which is a tetramer, is at least 0.65; this protein was also reported in error to contain half-occupied heme sites (*36*).

An additional point about the engineered enzyme is that the overexpression system generates polypeptide at a rate that apparently overruns the heme biosynthesis capacity of the bacteria grown in LB medium. Evidence for this comes from the fact that all preparations of the enzyme isolated from bacteria grown in LB broth without addition of other components contain a very large fraction of heme-deficient dimer. This dimer, which can be resolved from the holoenzyme on either ion exchange or hydrophobic chromatography media, exhibits an optical purity ratio of 0.38 *when fully purified*. The characterization of this purified enzyme as a dimer, and its reconstitution to fully active enzyme having an optical purity ratio equal to that of the holoenzyme (data not shown), also suggested that the "one heme per dimer" stoichiometry was incorrect. As explained above, the holoenzyme contains two hemes per dimer, and the actual heme-deficient dimeric material is an artifact of the overexpression of the polypeptide. We have found that addition of δ-aminolevulinic acid to LB growth medium greatly enhances the yield of holoenzyme, with heme-deficient enzyme no longer appearing in the isolate.

The purified enzyme runs as a single band of approximately 81 kDa on SDS−PAGE, while in native polyacrylamide electrophoresis gels, the native enzyme runs near the molecular weight of the dimer. Catalase and peroxidase activities of purified *M. tuberculosis* KatG are 4500 and 0.95 unit/mg, respectively. The catalase activity is twice as high as that reported by Johnsson et al. (*40*) or Regelsberger et al. (*32*), for overexpressed *M. tuberculosis* KatG and *Synechocystis* KatG, respectively. The peroxidase activity (*o*-dianisidine/*tert*-butyl hydroperoxide) measured here is close to that reported by these authors.

Spectral Properties of KatG. The optical spectrum of ferric (resting) *M. tuberculosis* KatG is the same as previously published spectra of this and other KatG enzymes, including that of wild-type *M. smegmatis* KatG (*36*, *41*).

In our efforts to characterize the structure of *M. tuberculosis* KatG, we are pursuing spectroscopic and enzymatic studies. A series of resonance Raman experiments were aimed at defining structural features of iron in the heme

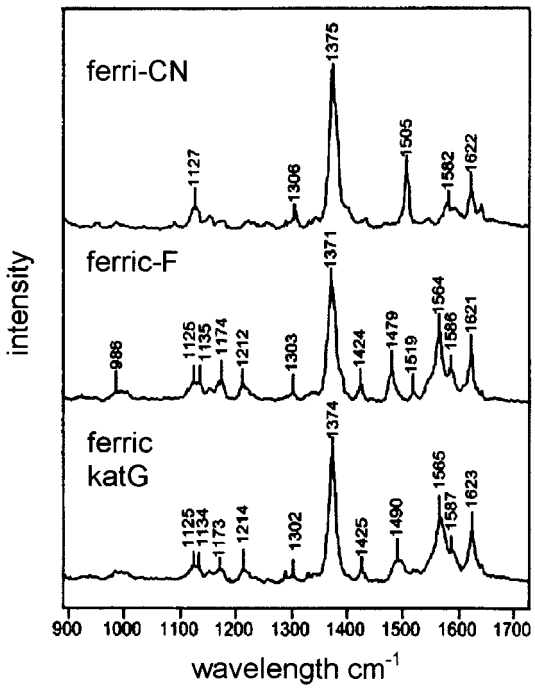

FIGURE 1: Resonance Raman spectra (high-frequency region) of native *M. tuberculosis* catalase-peroxidase (KatG), KatG-fluoride (ferric-F), and KatG-cyanide (ferric-CN).

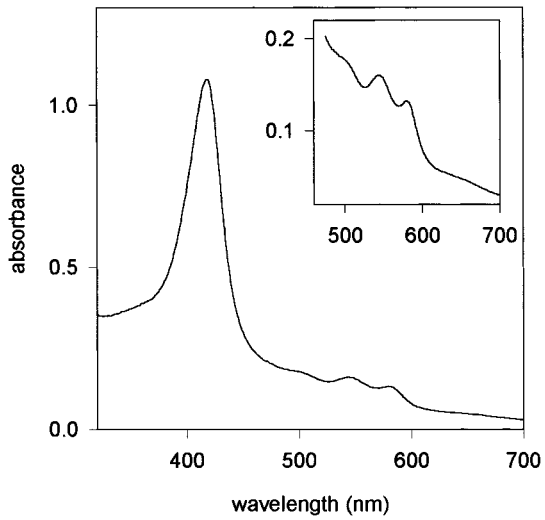

FIGURE 2: Optical (UV−visible) spectrum of the unstable intermediate formed from resting (ferric) *M. tuberculosis* KatG (10 μM) upon addition of excess H_2O_2 (in 20 mM potassium phosphate buffer, pH 7). The intermediate is identified as oxyferrous KatG (Compound III analogue). Inset: expanded visible region of the spectrum.

group. Figure 1 shows the high-frequency region of the resonance Raman spectrum of resting (ferric) *M. tuberculosis* KatG, along with spectra for the fluoride and cyanide complexes of the ferric enzyme. This experiment was designed to identify the spin state and coordination number of iron in the resting enzyme. The bands at 1565 (ν_{19}), 1490 (ν_3), and 1374 cm^{-1} (ν_4, oxidation-state marker band) occur near the frequencies of the same bands associated with five-coordinate heme in ferric peroxidases, including CCP (*42*), Mn-peroxidase (*43*), and *Streptomyces* sp. peroxidase (*44*). Fluoride binding to the native enzyme provides a six-coordinate high-spin form of KatG, which will exhibit new features that differentiate this form from the resting enzyme. The band at 1479 cm^{-1} (ν_3) for KatG−fluoride is typical of six-coordinate high-spin heme in other proteins (*45*). This band is missing from spectra of the native enzyme, indirectly confirming the five-coordinate nature of resting KatG.[2]

The binding of cyanide to the native enzyme provides a low-spin six-coordinate species. The band at 1640 cm^{-1} (ν_{10}) is typical for cyanide complexes of peroxidases (*43, 45, 46*) while the band at 1622 cm^{-1} [a vinyl vibrational band ($\nu_{C=C}$, vinyl II)] occurs near the frequency of the same band in other low-spin heme proteins. The small difference in frequency of this band between the resting, fluoride, and cyanide forms of KatG, however, warrants an additional comment: the frequency of this band in spectra of ferric KatG shifts in a manner analogous to its behavior in the equivalent forms of CCP, such that its position in the low-spin form is intermediate between its highest frequency in the spectrum of fresh resting enzyme and its lowest frequency in the high-spin, six-coordinate form (1621 cm^{-1}) (*42*−*45*).

Raman difference spectra in the high-frequency region, between the native enzyme and the enzyme in the presence of isoniazid, were examined since drug binding was observed to cause a small shift in the Soret absorbance maximum and extinction coefficient. These difference spectra did not reveal any changes. Also, no changes were detected in difference spectra for the ferrous-CO form of the enzyme in the presence and absence of the antibiotic (data not shown).

KatG Intermediates. Experiments were attempted to demonstrate Cmpd I formation from resting KatG plus hydrogen peroxide but could not identify optical changes typical of such a reaction in a peroxidase, under a variety of conditions used for stopped-flow spectrophotometry. For example, no significant absorbance changes were observed after mixing ferric KatG (10 μM) with concentrations of H_2O_2 less than 100 μM (data not shown). This is probably related to the high catalase activity of the enzyme and the very fast cycling of oxidized intermediates back to the ferric state of the resting enzyme. However, when very large excess of H_2O_2 (0.44 M) were used, the optical spectrum of the resting enzyme decayed in milliseconds. A spectrum with absorbance maxima at 418, 545, and 580 nm was then observed (Figure 2). The optical features of this intermediate, being in good agreement with those of oxyferrous HRP (Cmpd III) (*29, 47, 48*), allow assignment of this spectrum to oxyferrous KatG. The Cmpd III spectrum quickly disappears as the spectrum of the resting enzyme returns. These results suggest cycling of the ferric form through Cmpds I, II, and III under these conditions, but in contrast to the behavior of HRP, the oxyferrous enzyme is unstable. Thus, when excess peroxide is consumed in the catalytic reaction pathway, the ferric enzyme is regenerated.

In contrast to the results with hydrogen peroxide, alkyl peroxides such as *tert*-butyl hydroperoxide, 3-chloroperoxybenzoic acid, or peroxyacetic acid reacted with KatG to form an unstable species with optical characteristics similar to HRP Cmpd I. For example, reaction of KatG (10 μM) with

[2] The potential for KatG to behave like yeast cytochrome *c* peroxidase in terms of aging- and freezing-induced changes in coordination number and even spin state is possible given the homology between these peroxidases. Here, the predominant form of the enzyme at neutral pH (and high pH, data not shown) for freshly prepared KatG, that has never been frozen or exposed to glycerol, is the five-coordinate ferric species.

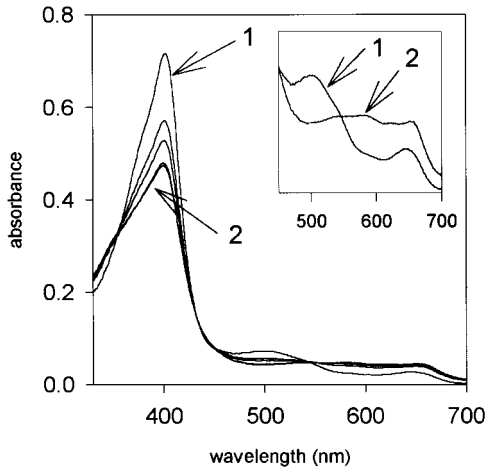

FIGURE 3: Absorption spectra showing the formation of KatG Cmpd I after addition of CPBA (100 μM) to resting catalase-peroxidase (10 μM) (in 20 mM phosphate buffer, pH 7): 1, resting KatG; 2, KatG Cmpd I. Inset: visible region of initial and final spectrum.

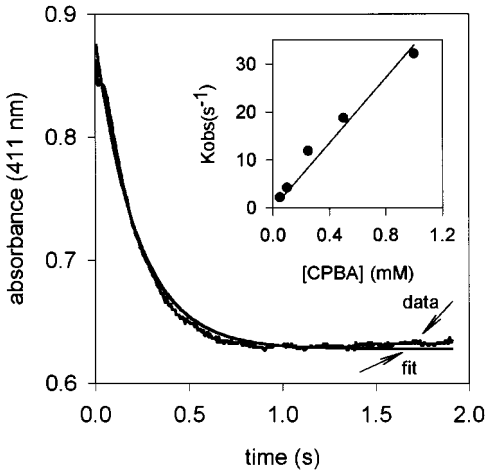

FIGURE 4: Absorbance vs time (recorded at 411 nm) showing formation of KatG Compound I (10 μM resting KatG with 100 μM CPBA, in 20 mM potassium phosphate buffer, pH 7). Also shown is a fit of the data to a first-order exponential rate equation. Inset: linear dependence of the observed rate constants (K_{obs}) as a function of concentration of 3-chloroperoxybenzoic acid (CPBA).

3-chloroperoxybenzoic acid (25 μM) or peroxyacetic acid (100 μM) or *tert*-butyl hydroperoxide (100 mM) generated the same optical intermediate taken to represent Cmpd I. (Stoichiometric equivalents of peroxides did not produce any optical changes.) Figure 3 shows optical stopped-flow data for a typical reaction (10 μM enzyme with 100 μM CPBA). The product spectrum (Figure 3, spectrum 2) is characterized by a decrease of approximately 40% in Soret intensity compared to the resting enzyme, with a λ_{max} at 411 nm. In the visible region, two new maxima appear, at 550 and 590 nm, with a shoulder at 655 nm. The decrease in Soret intensity for this product compared to ferric KatG is a typical optical change consistent with the change in oxidation state of the heme iron, while the shift in wavelength is less typical. The shift suggested that the intermediate may represent another form, at the oxidation level of Cmpd II, or possibly a complex formed between Cmpd I and excess CPBA or even chlorobenzoic acid. The decreased Soret extinction (and the finding that the λ_{max} is nearly identical for the product generated by the different peroxides), taken with the wavelengths of the maxima in the visible region, argues against these alternatives and in favor of Cmpd I. (A shift in the Soret to longer wavelengths was noted for KatG Cmpd I in the presence of large excesses of CPBA.) Identification of this intermediate as Cmpd I is confirmed using EPR spectroscopy (see below).

The rate of Cmpd I formation was determined from the time courses observed in stopped-flow experiments. Figure 4 shows the change in absorbance at 411 nm as a function of time for reaction of resting KatG with CPBA. Time domain data were fit (as shown) to single exponentials with K_{obs} equal to 4.26 s^{-1} under the conditions shown (10-fold excess of peroxide). The bimolecular rate constant for Cmpd I formation was determined from the slopes of the plots of K_{obs} versus the concentration of peroxide (Figure 4, inset, and Table 1). The rate constant using CPBA (3.1×10^4 M^{-1} s^{-1}) is 2-fold higher than that obtained using PAA (1.21×10^4 M^{-1} s^{-1}), while a much lower rate is found with tBOOH, which is likely due to the bulkiness of this peroxide.

The KatG Cmpd I intermediate was less stable in triethanolamine hydrochloride buffer (pH 7.8) than in phosphate buffer, possibly due to a reaction between the buffer and

Table 1: Rate Constants for Formation of Compound I and/or Compound II in *M. tuberculosis* KatG and HRP

conditions	Compound I ($M^{-1}s^{-1}$)	Compound II ($M^{-1}s^{-1}$)
KatG		
$+H_2O_2$[a]	ND[b]	
+tBOOH[a]	25.4	
+CPBA[a]	2.03×10^4	
+CPBA	3.1×10^4	
+PAA	1.21×10^4	
+CPBA + INH		ND
HRP		
$+H_2O_2$	0.93×10^7	
$+H_2O_2$ + INH		6.92×10^2

[a] In 10 mM TEA, pH 7.8; all others in 20 mM potassium phosphate buffer, pH 7. [b] ND, not determined.

Cpmd I (and/or a pH effect). Also, the apparent rate constant for Cmpd I formation was lower in TEA buffer at pH 7.8 than in phosphate buffer at pH 7 (Table 1). Small shifts in the maxima of the optical spectra of Cmpd I were also noted as a function of pH (data not shown).

KatG Cmpd I was unstable under the conditions used for its preparation from any of the peroxides, as evidenced by the relatively slow reappearance of the optical spectrum of the resting enzyme after incubation for a few seconds (Figure 5). The rate of reappearance of the ferric KatG spectrum was dependent on the peroxide concentration but was greater at lower concentrations of peroxide. This result suggests that there is recycling of the ferric enzyme in a reaction whose rate begins to compete with the rate of regeneration of Cmpd I from ferric enzyme, as peroxide is depleted. The instability of Cmpd I could result from electron-transfer reactions from endogenous or exogenous reductants that discharge it and restore the ferric enzyme in a classical peroxidase cycle. The fact that the reappearance of ferric enzyme occurs without the appearance of another intermediate suggested an instability for intermediates such as Cpmd II. This idea was confirmed in reactions described below, in which exogenous one-electron reductants were added to Cmpd I.

The identity of the species assigned as Cmpd I in the optical experiments was confirmed using low-temperature

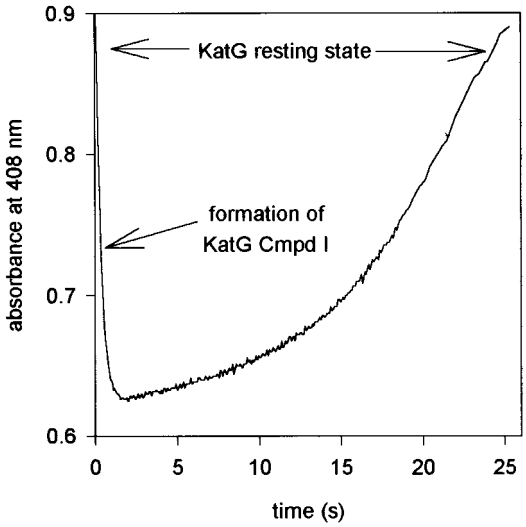

FIGURE 5: Extended absorbance vs time trace (at 408 nm) recorded after mixing 10 μM resting KatG with 100 μM CPBA (in 20 mM potassium phosphate buffer, pH 7).

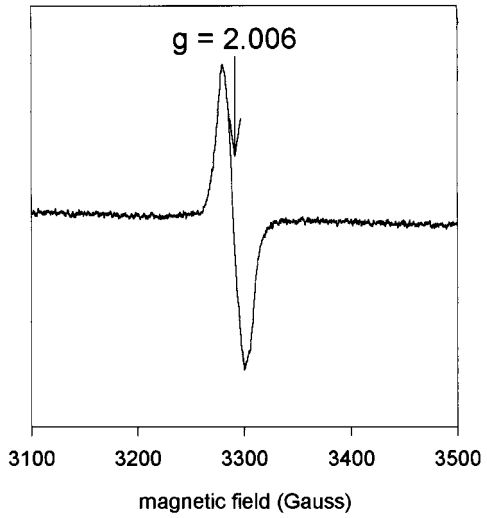

FIGURE 6: Low-temperature electron paramagnetic resonance spectrum of KatG Cmpd I. Resting KatG (100 μM) was mixed with PAA (1 mM) (both in 20 mM potassium phosphate buffer, pH 7), incubated for 10 s, and quickly frozen in liquid nitrogen. Spectrometer experimental conditions were as follows: scan time, 4 min; time constant, 0.3 s; temperature, 20 K; power, 5 mW; receiver gain, 2000; modulation amplitude, 0.63 G; frequency, 9.2367 GHz.

EPR spectroscopy (Figure 6). KatG was mixed with a 10-fold excess of PAA and was incubated for 10 s. The solution turned from brown to green immediately after mixing. The green solution was quickly frozen in liquid nitrogen as described under Experimental Procedures. No special conditions were required to observe the spectrum ($g = 2.006$), which was similar to that reported for Cmpd I of HRP (*29*, *47*, *48*) or catalase of *Proteus mirabilis* (*49*). The optical and EPR data taken together confirm the identity of KatG Cmpd I as a ferryl π-cation radical typical of peroxidase Cmpds I.

Having identified KatG Cmpd I, its reduction by substrates could be investigated. Ascorbate, potassium ferrocyanide, and also isoniazid were used in double-mixing stopped-flow experiments. KatG Cmpd I was prepared by mixing 10 μM KatG with 100 μM CBPA. After 4 s, which allows for conversion of all the resting enzyme to Cmpd I, each of these

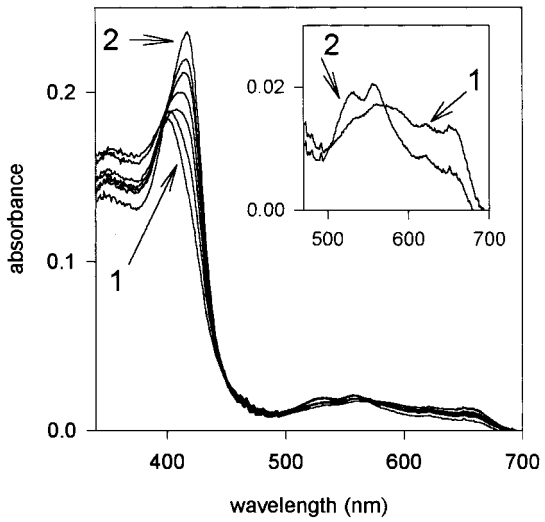

FIGURE 7: Absorption spectra showing formation of horseradish peroxidase Compound II after addition of isoniazid to Compound I. Compound I was formed by mixing resting horseradish peroxidase (10 μM) with 1 equiv of H_2O_2; isoniazid (150 μM) was added 3 s later: 1, HRP Compound I; 2, HRP Compound II. Inset: visible region of the initial and final spectra.

reductants (10-fold to 100-fold excess) was added in a second mixing step, and the optical changes were recorded. In each case, a rapid disappearance of Cmpd I occurred (severalfold more quickly than the rates in the absence of substrates) and the spectrum of ferric enzyme returned without detectable formation of intermediate(s) (Cmpd II) on the time scale accessible here. Therefore, no rate for reduction of Cmpd I was calculated. These results suggest that if a species analogous to Cmpd II is formed in KatG upon single-electron reduction of Cmpd I by these substrates, it is rapidly reduced further to the ferric state. Experiments described below, in which HRP was used in place of KatG, did, however, demonstrate that isoniazid achieves single-electron reduction of Cmpd I.

To compare the above results with the behavior of HRP, the formation of HRP Cmpd I and its reaction with isoniazid were investigated. As expected, the addition of 10 μM hydrogen peroxide to 10 μM HRP resulted in the quantitative oxidation of the resting enzyme to Cmpd I. This was confirmed by the optical spectrum of the intermediate, which contained features at wavelengths identical to the features reported by Blumberg et al. (*50*), and close to those reported by other authors (*51*, *52*) for HRP Cmpd I. The rate of Cmpd I formation was determined by fitting the optical changes at 401 nm to a single exponential. The calculated rate constant for formation of Cmpd I (0.93×10^7 M^{-1} s^{-1}) was close to values observed for native and mutated HRP in other reports (1×10^7 to 2×10^7 M^{-1} s^{-1}) (*53*). In contrast to the behavior of KatG, the formation of HRP Cmpd II from Cmpd I could be followed using isoniazid as a reductant. Figure 7 shows Cmpd II generation from HRP Cmpd I upon reaction with the drug. Resting HRP (10 μM) was first mixed with 10 μM H_2O_2. After 3 s, excess isoniazid was added in a second mixing step. The new intermediate, which does not decay rapidly under these conditions, is characterized by a Soret peak at 418 nm and two bands at 531 and 557 nm (Figure 7, inset), all typical of HRP Cmpd II (*50*). It was also possible to observe the formation of the same species using a small excess of H_2O_2 added to resting HRP (data not shown). The

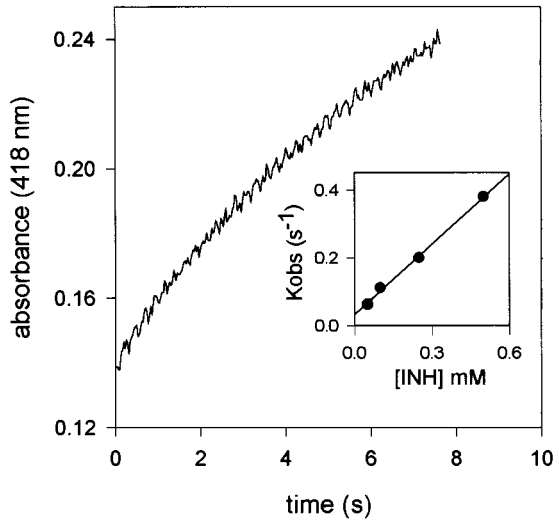

FIGURE 8: Absorbance vs time trace (at 418 nm) for horseradish peroxidase Compound II formation from Compound I. Inset: linear dependence of the observed rate constants (K_{obs}) as a function of isoniazid concentration, obtained from fitting data to an exponential first-order rate equation.

second-order rate constant for HRP Cmpd II formation from Cmpd I plus isoniazid was determined from K_{obs} (obtained from the time courses recorded at 418 nm) versus the concentration of INH (Figure 8). Consistent with a previous report, the apparent second-order reaction rate for the reaction of HRP Cmpd I with INH is 6.92×10^2 M^{-1} s^{-1} (*54*).

DISCUSSION

Isonicotinic acid hydrazide (INH) is among the arsenal of primary antibiotic drugs currently used in the treatment of *M. tuberculosis* infections. The appearance of many isoniazid-resistant strains that carry a mutation in the *katG* gene continues to drive research efforts aimed at understanding catalase-peroxidase structure and function, and the mechanism of drug oxidation. Isoniazid action against mycobacteria is believed to require oxidative activation. In vitro oxidation of isoniazid by catalase-peroxidase has been demonstrated to occur through several routes that could provide a catalytic oxidant, though there has not been a focus on classical peroxidase chemistry initiated by peroxide action on the ferric enzyme. The current report, which provides some characterization of the resting enzyme, also addressed the kinetics of reaction of *M. tuberculosis* KatG with peroxides and substrates including the antibiotic isoniazid.

The results for overexpressed *M. tuberculosis* KatG confirmed that pure enzyme contains one heme per monomer in a dimer, and illustrates that the low optical purity ratio for catalase-peroxidases reported in the literature arises from a high extinction coefficient for the polypeptide rather than a low heme content. The resonance Raman results on the ferric enzyme confirmed that resting KatG contains five-coordinate high-spin iron, and also showed that no changes in iron coordination number or spin state could be detected in response to binding of the antibiotic isoniazid. For HRP, it has been shown that the binding of some substrates, such as benzhydroxamic acid (BHA), induces a change in iron coordination number from 5 to 6, while hydroquinone does not (*55*). This phenomenon reflects the binding of a water ligand that accompanies the binding of BHA. For KatG, NMR spectroscopy has shown that isoniazid binds approximately 12 Å from the heme iron (*56*). Drug binding to resting KatG also induces a small change in intensity and wavelength of the Soret peak suggested to be related to a change in iron coordination number from 6 to 5 for a subpopulation of the enzyme (*56*). The Raman difference spectra reported above could not confirm a change in coordination number for freshly prepared *M. tuberculosis* KatG in the presence compared to the absence of isoniazid. A large difference in optical extinction coefficients for the two forms, however, with a small fractional conversion of six- to five-coordinate species upon binding of the drug, might explain the apparent lack of agreement between optical and Raman measurements. It was also found that the Raman spectra of the ferrous-CO form of KatG in the presence and absence of isoniazid were indistinguishable, consistent with conservation of heme cavity structure in response to drug binding.

M. tuberculosis KatG has high catalase activity (4500 units/mg), in agreement with previous work (*32*, *40*). It also has significant peroxidase catalytic activity, which will allow the enzyme to oxidize a variety of electron donors. Stopped-flow measurements showed that under conditions expected to initiate a peroxidase cycle in KatG with hydrogen peroxide, no Cmpd I could be detected on the millisecond time scale. On the other hand, addition of large excesses of H_2O_2 led to the formation of KatG Cmpd III (oxyferrous KatG), which is also unstable. The routes to Cmpd III may include reaction of the ferryl form (Cmpd II) with hydrogen peroxide as in HRP (*23*), but no intermediates in the in KatG reaction using excess hydrogen peroxide could be detected here.

Results with other peroxides demonstrate formation of an unstable oxyferryl porphyrin π-cation-radical Cmpd I analogue in KatG (*26*). Its rate of formation depended on the nature of the peroxide used, its concentration, and the pH, while it decayed to the resting enzyme with no intermediates detectable. The stopped-flow measurements for the reaction of KatG Cmpd I with INH, ascorbate, or potassium ferrocyanide showed that KatG Cmpd I decay is greatly accelerated by these single-electron reductants. It is likely that these reductants reduce Cmpd I to Cmpd II, and that Cmpd II is reduced to the ferric enzyme too fast for observation in these measurements. Whether the mechanism involves a second single-electron reaction by isoniazid (or an isoniazid radical) or an endogenous reductant is therefore unclear at present. Certain peroxidases, including ascorbate peroxidase and fungal peroxidase, behave in a similar manner, reflecting an unstable Cmpd II (*57*, *58*). The finding that HRP Cmpd II *is* generated in the reaction of HRP Cmpd I with isoniazid demonstrates that the drug may be considered a bona fide single-electron peroxidase substrate. These results point to the operation of a classical peroxidase pathway for the oxidation of isoniazid by KatG, though proof for the intermediacy of Cmpd II awaits further study.

While our work was in progress, a report on a fungal KatG appeared, demonstrating the formation of Cmpd II upon reduction of Cmpd I by ascorbate and other substrates (*32*). The assignment of the Cmpd II optical spectrum, however, is questionable in the report since neither the Soret peak nor the features in the visible region match those of ferryl HRP or ferryl CCP.

Other studies of KatG have presented evidence for drug oxidation initiated by superoxide and the ferric enzyme (*34*), and evidence for a pathway initiated by reduction of the ferric enzyme under aerobic conditions (*33*). A variety of products are known to be produced during these oxidation reactions, in different proportions depending on the initiation pathway. These facts, taken with the finding that KatG Cmpd I returns to the ferric enzyme spontaneously, and that Cmpd II is apparently unstable, make it likely that the classical peroxidase cycle, in which 2 mol of substrate undergoes identical single-electron oxidations catalyzed by Cmpds I and II, may be inadequate for describing this system. Also, the hypervalent KatG intermediates could differ in their redox potentials and thereby catalyze more than one substrate oxidation reaction step.

In order for superoxide binding to the ferric enzyme or reduction to the ferrous enzyme followed by oxygenation to be important initiating steps in drug oxidation in vivo, the instability of the resulting oxyferrous enzyme requires a very rapid second electron transfer step to attain the Cmpd I oxidation state by these routes. Our results demonstrated an apparently spontaneous and rapid decomposition of oxyferrous KatG, but information about the rates of further reactions of oxyferrous KatG is not yet available.

Mycobacteria reside in macrophages after infection of the host, and are exposed to the reactive oxygen and nitrogen intermediates produced by phagolysosomal membranes. Little is known about the chemical processes that ensue in and around the resident bacteria, but it has been shown that mycobacteria are relatively resistant to hydrogen peroxide, and even peroxynitrite (*59*). Catalase and peroxynitritase activities of KatG are likely to contribute to this protection (*60*). Also important is the issue of how well the mycobacterial cell wall protects the cell from the reactive oxygen and nitrogen intermediates. This raises the question of whether the function of KatG in the extracellular space (that is, outside the bacterium but within the macrophage) is important in vivo. KatG has been shown to be secreted by mycobacteria (*61*, *62*), making this a possibility that would allow access of potential initiators, such as superoxide and peroxides, to ferric KatG. A better understanding of these issues is needed to address the mechanism of KatG function in infected hosts and the relevance of the importance of various pathways for activation of isoniazid.

ACKNOWLEDGMENT

We thank Dr. Charlotte Russell, City College of The City University of New York, for suggesting the addition of δ-aminolevulinic acid to bacterial growth media.

REFERENCES

1. Robitzek, E. H., and Selikoff, I. J. (1952) *Annu. Rev. Tuberc. 65*, 402−410.
2. Middlebrook, G., Cohn, M. L., and Schaefer, W. B. (1954) *Annu. Rev. Tuberc. 70*, 852−872.
3. Zhang, Y., Heym, B., Allen, B., Young, D., and Cole, S. (1992) *Nature 358*, 591−593.
4. Johnsson, K., and Schultz, P. G. (1994) *J. Am. Chem. Soc. 116*, 7425−7426.
5. Johnsson, K., King, D. S., and Schultz, P. G. (1995) *J. Am. Chem. Soc. 117*, 5009−5010.
6. Zhang, Y., Garbe, T., and Young, D. (1993) *Mol. Microbiol. 8*, 521−524.
7. Heym, B., and Cole, S. T. (1997) *Int. J. Antimicrob. Agents 8*, 61−70.
8. Heym, B., Honore, N., Truffot-Pernot, C., Banerjee, A., Schurra, C., Jacobs, W. R., Jr., van Embden, J. D., Grosset, J. H., and Cole, S. T. (1994) *Lancet 344*, 293−298.
9. Musser, J. M. (1995) *Clin. Microbiol. Rev. 8*, 496−514.
10. Musser, J. M., Kapur, V., Williams, D. L., Kreiswirth, B. N., van Soolingen, D., and van Embden, J. D. (1996) *J. Infect. Dis. 173*, 196−202.
11. Rouse, D. A., DeVito, J. A., Li, Z., Byer, H., and Morris, S. L. (1996) *Mol. Microbiol. 22*, 583−592.
12. Quemard, A., Sacchettini, J. C., Dessen, A., Vilcheze, C., Bittman, R., Jacobs, W. R., Jr., and Blanchard, J. S. (1995) *Biochemistry 34*, 8235−8241.
13. Quemard, A., Dessen, A., Sugantino, M., Jacobs, W. R. J., Sacchettini, J. C., and Blanchard, J. S. (1996) *J. Am. Chem. Soc. 118*, 1561−1562.
14. Basso, L. A., Zheng, R., and Blanchard, J. S. (1996) *J. Am. Chem. Soc. 118*, 11301−11302.
15. Banerjee, A., Duvnau, E., Quemard, A., Balasubramanian, V., Sun Um, K., Wilson, T., Collins, D., Lisle, G., and Jacobs, W. R. J. (1994) *Science 263*, 227−230.
16. Rozwarski, D. A., Grant, G. A., Barton, D. H. R., Jacobs, W. R., Jr., and Sacchettini, J. C. (1998) *Science 279*, 98−102.
17. Mdluli, K., Slayden, R. A., Zhu, Y., Ramaswamy, S., Pan, X., Mead, D., Crane, D. D., Musser, J. M., and Barry, C. E., 3rd (1998) *Science 280*, 1607−1610.
18. Welinder, K. G. (1991) *Biochim. Biophys. Acta 1080*, 215−220.
19. Dawson, J. H. (1988) *Science 240*, 433−439.
20. Kaim, W., and Schwederski, B. (1991) in *Bioinorganic Chemistry*, Wiley, Chichester, U.K.
21. Schulz, C. E., Devaney, P. W., Winkler, H., Debrunner, P. G., Doan, N., Chiang, R., Rutter, R., and Hager, L. P. (1979) *FEBS Lett. 103*, 102−105.
22. Moss, T. H., Ehrenberg, A., and Bearden, A. J. (1969) *Biochemistry 8*, 4159−4162.
23. Dunford, H. B. (1991) in *Peroxidases in Chemistry and Biology* (Everse, J., Everse, K. E., and Grisham, M. B., Eds.) pp 1−25, CRC Press, Boca Raton, FL.
24. Yonetani, T., and Anni, H. (1987) *J. Biol. Chem. 262*, 9547−9554.
25. English, A. M., and Tsaprailis, T. (1995) in *Advances in Inorganic Chemistry*, pp 79−125, Academic Press, New York.
26. Erman, J. E., Vitello, L. B., Mauro, J. M., and Kraut, J. (1989) *Biochemistry 28*, 7992−7995.
27. Ricard, J., and Nari, J. (1967) *Biochim. Biophys. Acta 132*, 321−329.
28. Fishel, L. A., Farnum, M. F., Mauro, J. M., Miller, M. A., Kraut, J., Liu, Y. J., Tan, X. L., and Scholes, C. P. (1991) *Biochemistry 30*, 1986−1996.
29. Sanders, B. C., Holmes-Siedle, A. G., and Stark, B. P. (1964) in *Peroxidase*, pp 200−238, Butterworths, Washington, DC.
30. Chance, B. (1952) *Arch. Biochem. Biophys. 41*, 405−415.
31. Chance, B. (1952) *Arch. Biochem. Biophys. 41*, 416−423.
32. Regelsberger, G., Jakopitsch, C., Engleder, M., Ruker, F., Peschek, G. A., and Obinger, C. (1999) *Biochemistry 38*, 10480−10488.
33. Magliozzo, R. S., and Marcinkeviciene, J. A. (1996) *J. Am. Chem. Soc. 188*, 11303−11304.
34. Wengenack, N. L., Hoard, H. M., and Rusnak, F. (1999) *Biochemistry 121*, 9748−9749.
35. Magliozzo, R. S., and Marcinkeviciene, J. A. (1997) *J. Biol. Chem. 272*, 8867−8870.
36. Marcinkeviciene, J. A., Magliozzo, R. S., and Blanchard, J. S. (1995) *J. Biol. Chem. 270*, 22290−22295.
37. Beers, R. F., and Sizers, I. W. (1952) *J. Biol. Chem. 195*, 133−140.
38. Falk, J. K. (1964) in *Porphyrin and Metalloporphyrins* (Smith, K. M., Ed.) pp 804−807, Elsevier Publishing Co, New York.
39. Nagy, J. M., Cass, A. E., and Brown, K. A. (1997) *J. Biol. Chem. 272*, 31265−31271.
40. Johnsson, K., Froland, W. A., and Schultz, P. G. (1997) *J. Biol. Chem. 272*, 2834−2840.

41. Gill, S. C., and von Hippel, P. H. (1989) *Anal. Biochem. 182*, 319−326.
42. Dasgupta, S., Rousseau, D. L., Anni, H., and Yonetani, T. (1989) *J. Biol. Chem. 264*, 654−662.
43. Mino, Y., Wariishi, H., Blackburn, N. J., Loehr, T. M., and Gold, M. H. (1988) *J. Biol. Chem. 263*, 7029−7036.
44. Youn, H. D., Yim, Y. I., Kim, K., Hah, Y. C., and Kang, S. O. (1995) *J. Biol. Chem. 270*, 13740−13747.
45. Andersson, L. A., Renganathan, V., Chiu, A. A., Loehr, T. M., and Gold, M. H. (1985) *J. Biol. Chem. 260*, 6080−6087.
46. Felton, R. H., and Yu, N. T. (1978) in *The Porphyrins* (Dolphin, D., Ed.) pp 347−393, Academic Press, New York.
47. Goodwin, D. C., Grover, T. A., and Aust, S. D. (1997) *Biochemistry 36*, 139−147.
48. Wittenberg, J. B., Noble, R. W., Wittenberg, B. A., Antonini, E., Brunori, M., and Wyman, J. (1967) *J. Biol. Chem. 242*, 626−634.
49. Ivancich, A., Jouve, H. M., Sartor, B., and Gaillard, J. (1997) *Biochemistry 36*, 9356−9364.
50. Blumberg, W. E., Peisach, J., Wittenberg, B. A., and Wittenberg, J. B. (1968) *J. Biol. Chem. 25*, 1854−1862.
51. Savenkova, M. I., Kuo, J. M., and Ortiz de Montellano, P. R. (1998) *Biochemistry 37*, 10828−10836.
52. Hewson, W. D., and Hager, L. P. (1979) *J. Biol. Chem. 254*, 3182−3186.
53. Morimoto, A., Tanaka, M., Takahashi, S., Ishimori, K., Hori, H., and Morishima, I. (1998) *J. Biol. Chem. 273*, 14753−14760.
54. Rodriguez-Lopez, J. N., Hernandez-Ruiz, J., Garcia-Canovas, F., Thorneley, R. N., Acosta, M., and Arnao, M. B. (1997) *J. Biol. Chem. 272*, 5469−5476.
55. Teraoka, J., and Kitagawa, T. (1981) *J. Biol. Chem. 256*, 3969−3977.
56. Wengenack, N. L., Todorovic, S., Yu, L., and Rusnak, F. (1998) *Biochemistry 37*, 15825−15834.
57. Farhangrazi, Z. S., Copeland, B. R., Nakayama, T., Amachi, T., Yamazaki, I., and Powers, L. S. (1994) *Biochemistry 33*, 5647−5652.
58. Mandelman, D., Jamal, J., and Poulos, T. L. (1998) *Biochemistry 37*, 17610−17617.
59. Yu, K., Mitchell, C., Xing, Y., Magliozzo, R. S., Bloom, B. R., and Chan, J. (1999) *Tuberc. Lung Disease 79*, 191−198.
60. Wengenack, N. L., Jensen, M. P., Rusnak, F., and Stern, M. K. (1999) *Biochem. Biophys. Res. Commun. 256*, 485−487.
61. Sonnenberg, M. G., and Belisle, J. T. (1997) *Infect. Immun. 65*, 4515−4524.
62. Raynaud, C., Etienne, G., Peyron, P., Laneelle, M. A., and Daffe, M. (1998) *Microbiology 144*, 577−587.

BI0005815